Solution Structure and Dynamics of a Heat Shock Protein Assembly Probed by Hydrogen Exchange and Mass Spectrometry†

Patrick L. Wintrode,‡ Kenneth L. Friedrich,§ Elizabeth Vierling,§ Jean B. Smith,‡ and David L. Smith*,‡

Nebraska Center for Mass Spectrometry, Department of Chemistry, University of Nebraska, Lincoln, Nebraska 68588, and Department of Biochemistry and Molecular Biophysics, University of Arizona, Tucson, Arizona 85721

Received January 21, 2003; Revised Manuscript Received June 23, 2003

ABSTRACT: The solution conformation and dynamics of the 16.9 kDa small heat shock protein from wheat have been studied using a combination of hydrogen/deuterium exchange, proteolytic digestion, and mass spectrometry. At room temperature, HSP16.9 exists as a dodecameric assembly. Regions of HSP16.9 that form extensive and essential intersubunit contacts in the assembly, including residues 1−40 and 131−151, show little or no protection against hydrogen/deuterium exchange after incubation in D_2O for 5 s. The high levels of hydrogen/deuterium exchange indicate that these regions have experienced large conformational fluctuations in solution, breaking intersubunit contacts and exposing buried amide hydrogens to solvent. When HSP16.9 is pulse labeled for 10 ms, residues 1−40 and 131−151 are substantially more protected than they are after 5 s. Thus, the breaking of intersubunit contacts occurs on a time scale between 10 milliseconds and 5 s. At 42 °C, HSP16.9 exists in a suboligomeric form. When the intrinsic temperature dependence of hydrogen/deuterium exchange is taken into account, exchange patterns at 25 and 42 °C are identical within experimental error, suggesting that the conformation of individual HSP16.9 subunits is the same in both the dodecameric and subdodecameric forms. Significant protection is seen in regions that form the dimeric interface, suggesting that the stable suboligomeric form is a dimer. Taken together, these results suggest that heat activation of HSP16.9 occurs by shifting the dodecamer ↔ dimer equilibrium in favor of free dimers. The conformation of the dimers themselves does not appear to be altered with an increase in temperature.

Small heat shock proteins (sHSPs)[1] are a class of molecular chaperones that have a very large capacity for binding denatured proteins and preventing their aggregation (*1*). sHSPs are found in plants, animals, eubacteria, and archea bacteria. In animals, sHSPs have broad tissue distributions and complex expression patterns. The family includes the α-crystallins, which are important structural components of the vertebrate eye lens (*1*). Unlike the better known molecular chaperones GroEL and DnaK, sHSPs cannot refold denatured proteins. However, it has been demonstrated that when denatured proteins bound to sHSPs are mixed with the DnaK chaperone system and ATP, they can be successfully refolded. According to the current working model for sHSP action, sHSPs bind to denatured proteins present in thermally stressed cells by trapping them in a nonnative but refoldable state. These sHSP-bound proteins are then transferred to the DnaK system for refolding (*1*). Additionally, sHSPs may associate with cellular membranes during heat stress and may be involved in regulating membrane fluidity (*2*).

sHSPs exist as large assemblies, ranging in size from 9 to 24 monomers depending on the particular protein species. The three-dimensional structure of the 16.9 kDa sHSP from *Triticum aestivum* (wheat) has recently been determined by X-ray crystallography (*3*). HSP16.9 exists as an assembly of 12 monomers arranged in two rings, each consisting of three dimers. The monomer consists of a β-sandwich formed from two β-sheets, one composed of β-strands 2, 3, 9, and 8 and the other of β-strands 7, 5, and 4. This β-sandwich motif is seen in other sHSPs and is termed the α-crystallin domain. Connecting strands 5 and 7 is an extended loop formed by residues 83−105 which contains a short β-strand (β6). This loop comprises the major part of the dimer interface, interacting with the first β-sheet of the partner monomer. Essential contacts between dimers are formed by the 40 N-terminal residues, which form pairs of intertwining α-helical domains. The 40 N-terminal residues are resolved in only 6 of the 12 monomers. In the other six, they do not appear in the electron density, indicating that they are highly dynamic and/or disordered. The 10 C-terminal residues are also involved in important interdimer contacts.

The ability of sHSPs to bind denatured proteins is activated by elevated temperatures (*1*, *4*). While the dodecameric form of HSP16.9 predominates at room temperature, above ∼35 °C, this assembly breaks down, and much smaller species predominate (*3*). These smaller species, which appear to constitute the activated form of HSP16.9, are not as well characterized as the dodecameric form. In other sHSP

† Supported by NIH Grants RO1 EY07609 and RO1 GM42762.

* To whom correspondence should be addressed: Department of Chemistry, University of Nebraska, Lincoln, NE 68588. E-mail: dsmith7@unl.edu.

‡ University of Nebraska.

§ University of Arizona.

[1] Abbreviations: sHSPs, small heat shock proteins; HSP16.9, small heat shock protein 16.9; HSP18.1, small heat shock protein 18.1; HPLC, high-pressure liquid chromatography; H/D, hydrogen/deuterium; ESIMS, electrospray ionization mass spectrometry; ANS, 1-anilinonaphthalene-8-sulfonic acid; DEAE, diethylaminoethyl-Sephadex.

10.1021/bi034117m CCC: $25.00
Published on Web 08/20/2003

systems, ANS binding has revealed that increased temperatures lead to exposure of hydrophobic surface area presumably involved in substrate binding (*5*). The nature of the conformational change(s) responsible for exposing this surface area is unknown, but has been suggested to result, at least in part, from oligomer dissociation (*3*).

Additionally, when the HSP16.9 oligomer is incubated in the presence of the related HSP18.1, hybrid assemblies containing subunits from both species form within several minutes at room temperature (*3*). This exchange indicates that, despite its stability under crystallization conditions, in solution the dodecameric form of HSP16.9 is in rapid equilibrium with smaller subassemblies. A recent study monitored the kinetics and stoichiometry of subunit exchange between HSP16.9 and HSP18.1 (*6*). Results indicate that, after 4 min, the major species consists of hybrid complexes in which HSP16.9 and HSP18.1 have exchanged two monomers, suggesting that the dodecamer is in rapid equilibrium with free dimers. Beyond this, little is known about the conformation of HSP16.9 when it is removed from the dodecamer. In particular, it is not known to what extent HSP16.9 monomers in these smaller assemblies retain the structure that they adopt in the complete dodecamer.

A powerful technique for studying the structure and dynamics of proteins in solution is amide hydrogen/deuterium exchange (*7*). In these experiments, hydrogen/deuterium (H/D) exchange rates of backbone amide hydrogens are measured following incubation of proteins in D_2O. It is believed that an amide hydrogen must be exposed to solvent to exchange. Amide hydrogens not involved in hydrogen bonding and located on the protein surface or in unstructured regions will exchange very rapidly, typically within several seconds at pH 7. If an amide hydrogen is buried in the protein interior or participates in hydrogen bonding, it will exchange only if fluctuations occur that disrupt its interactions with neighboring groups and expose it to solvent. The exchange process for such amide hydrogens may be described by the model (*8*)

$$\text{closed(H)} \underset{k_{-1}}{\overset{k_1}{\rightleftharpoons}} \text{open(H)} \xrightarrow{k_{\text{int}}} \text{open(D)} \underset{k_1}{\overset{k_{-1}}{\rightleftharpoons}} \text{closed(D)}$$

where the closed state is the form in which the amide hydrogen is buried or hydrogen bonded and the open state is the form in which it is exposed to solvent and available for exchange. In this model, k_1 and k_{-1} are the rate constants for the opening and closing process(es), respectively, and k_{int} is the intrinsic rate of H/D exchange for an exposed amide hydrogen. For most proteins under native conditions, $k_{-1} \gg k_{\text{int}}$, and therefore, the observed rate of hydrogen exchange can be expressed as

$$k_{\text{obs}} = \frac{k_1}{k_{-1}} k_{\text{int}} = K_{\text{eq}} k_{\text{int}}$$

Different aspects of protein structure and dynamics can be probed depending on how the H/D exchange experiment is carried out. Transiently exposing a protein to D_2O for a few seconds will identify folded and unfolded regions. By continuously incubating a protein in D_2O and measuring the extent of exchange as a function of time, one obtains an observed rate constant that is related to the degree to which different regions experience fluctuations that disrupt their structure.

Traditionally, local hydrogen exchange rates could be measured only by NMR spectroscopy, but in recent years, it has been demonstrated that localized exchange rates can also be measured by mass spectrometry (*9*). When combined with proteolytic digestion, mass spectrometry can identify regions of a protein exhibiting different exchange rates. Mass spectrometry also allows hydrogen exchange measurements on proteins that are too large or too insoluble to be studied by NMR. In addition, mass spectrometry may resolve populations of proteins that adopt different conformations.

We have used hydrogen exchange and mass spectrometry to study the structure and dynamics of HSP16.9 at room temperature and at elevated temperatures. Combining proteolytic digestion with hydrogen exchange and mass spectrometry has enabled us to characterize, for the first time, the local dynamics of an sHSP assembly in solution.

METHODS

Preparation of sHSP16.9. Wild-type *T. aestivum* (wheat) HSP16.9 (plasmid AZ388) was expressed as a recombinant protein in *Escherichia coli* BL21 cells (Novagen) and then purified to >95% homogeneity by conventional methods as described by Lee *et al.* (*10*) with the following modification. After ammonium sulfate precipitation, sucrose gradient centrifugation, and DEAE chromatography, an additional step was added to the purification. The fractions from the DEAE column were loaded on a hydroxyapatite column, which was developed with a gradient of 10 to 400 mM $NaPO_4$ (pH 7.5). HSP16.9 eluted at approximately 380 mM $NaPO_4$. The protein was concentrated and stored in 25 mM $NaPO_4$ (pH 7.5).

Hydrogen Exchange. Hydrogen/deuterium exchange was initiated by diluting 5 μL of HSP16.9 [0.25 mM HSP16.9 monomer in 10 mM potassium phosphate (pH 7.0)] 20-fold into the labeling solution [D_2O and 5 mM potassium phosphate (pH 7.0)]. Incubation times ranged from 5 s to 165 min. Exchange was quenched by mixing the solution in a 1:1 ratio with an ice-cold solution of 100 mM potassium phosphate (pH 2.5).

Rapid pulsed labeling was carried out using a Bio-Logic QM-5 continuous quench-flow apparatus. The labeling solution consisted of D_2O and 5 mM phosphate (pH 9.5). The quench solution was as described above. HSP16.9 was diluted 20-fold into D_2O; the exchange was quenched after 10 ms by mixing at a 1:1 ratio with quench buffer, and the solution was immediately put on dry ice.

Isotope Analysis by HPLC−ESIMS. The sample was applied to a column of immobilized pepsin using H_2O and 0.05% TFA as the mobile phase. The column dimensions were 2 mm × 5 cm, and the flow rate was 200 μL/min. From the pepsin column, digested protein was collected in a micropeptide trap and washed for 1 min at a rate of 200 μL/min. Material in the trap was then eluted onto a microbore C18 HPLC column coupled to a Finnigan LCQ quadrupole ion trap mass spectrometer. Peptides were eluted from the column in 10 min using a gradient of 20 to 35% acetonitrile at a flow rate of 50 μL/min. The pepsin column, micropeptide trap, and C18 column were all immersed in ice during the entire procedure.

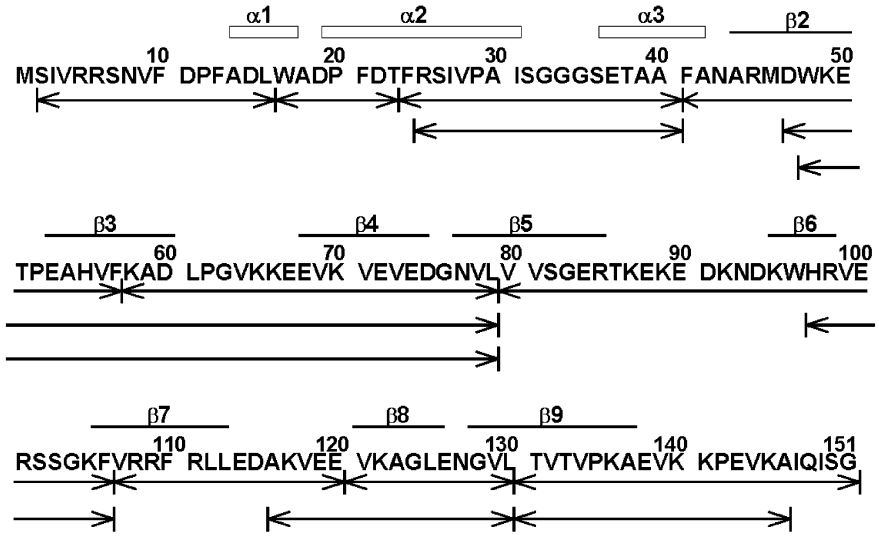

FIGURE 1: Amino acid sequence of HSP16.9. Secondary structure is indicated above the sequence. Lines under the sequence identify peptic fragments identified by MS/MS.

The extent of deuterium incorporation was determined from the shift in mass of labeled peptides relative to unlabeled peptides. Peptide masses were computed from the centroid of the isotopic envelope using MagTran software. To correct for deuterium loss during analysis, a fully deuterated reference sample was prepared by incubating HSP16.9 in D_2O (pH 2.5) at room temperature for 24 h. The extent of deuterium incorporation, corrected for back exchange, was calculated according to eq 1.

$$D = \frac{m - m_{0\%}}{m_{100\%} - m_{0\%}} \times N \quad (1)$$

where m is the mass of the sample being analyzed, $m_{100\%}$ is the mass of the fully deuterated reference sample, $m_{0\%}$ is the mass of the undeuterated reference sample, and N is the total number of exchangeable amide hydrogens in the peptide. Repeat experiments indicate an average error in the corrected deuteration level of ±5%.

Deuteration level *versus* time curves for each peptide were fit to the expression $y = N_1e^{-k_1X} + N_2e^{-k_2X} + N_3e^{-k_3X}$, where N_1-N_3 are the number of fast, intermediate, and slow exchanging amide hydrogens, respectively, and k_1-k_3 are the corresponding rate constants for exchange (*9*). Nonlinear least-squares fitting was carried out using the program Kaleidagraph. Prior to the H/D exchange studies, peptides resulting from the pepsin digest of HSP16.9 were identified by collision-induced dissociation MS/MS.

RESULTS

Identification of Peptides. On-line pepsin digestion followed by HPLC separation and tandem MS/MS led to identification of 16 peptides that completely covered the sequence of HSP16.9 (Figure 1). Peptides ranged in size from 7 to 30 amino acids. The average peptide size was 16 amino acids.

Continuous D_2O Labeling at 25 °C. In terms of exchange behavior, the 16 peptides cluster into several classes, corresponding to contiguous regions of the HSP16.9 sequence. In the analysis below, we will focus on 13 largely nonredundant peptides. Exchange data for representative peptides from regions with different exchange behavior are presented in Figure 2a. To illustrate more clearly the differences in exchange at the early time points, the same data for the first 200 s only are shown in Figure 2b.

Deuteration level *versus* time curves were fit to a sum of three exponentials, allowing the amide hydrogens in each peptide to be separated into three classes based on their exchange rates. This fitting identified distinct exchange behaviors that differed from each other by several orders of magnitude. Exchange rate constants of $>0.1\ s^{-1}$ are classified as fast, those equal to $\sim0.001\ s^{-1}$ as intermediate, and those of $<1.0 \times 10^{-5}\ s^{-1}$ as slow. The number of fast, intermediate, and slow exchanging amide hydrogens in each peptide, along with their rates, are given in Table 1. The rates for fast exchanging amide hydrogens are on the same order of magnitude (within a factor of ~3 to ~8) as the intrinsic exchange rates for unprotected amide hydrogens calculated according to Bai and Englander (*11*). The rates for slow exchanging amide hydrogens are 10^{-5} times slower than the calculated intrinsic exchange rates. It should be noted that, since the maximum exchange time was 2.75 h, these numbers represent only an upper limit for the rate constants of the slowly exchanging amide hydrogens.

Deuterium levels mapped onto the three-dimensional structure of HSP16.9 are shown in Figure 3. The fastest exchanging peptides comprise residues 2−40. Peptides from this region are 80−85% exchanged after 5 s and 85−90% exchanged after 10 s. In the crystal structure of HSP16.9, residues 2−40 exist in two distinct populations (*3*). In half of the 12 monomers, these residues are absent from the electron density map, indicating that they are highly dynamic or disordered. This lack of structure is consistent with the low level of protection that is observed for this region. However, in the other six monomers, residues 2−40 form extensive intersubunit contacts and α-helical structure.

In addition, they are largely buried in the interior of the ring formed by the assembly. Nonetheless, even for the shortest labeling time, peptides from this region exhibit only a single peak corresponding to the essentially unprotected form.

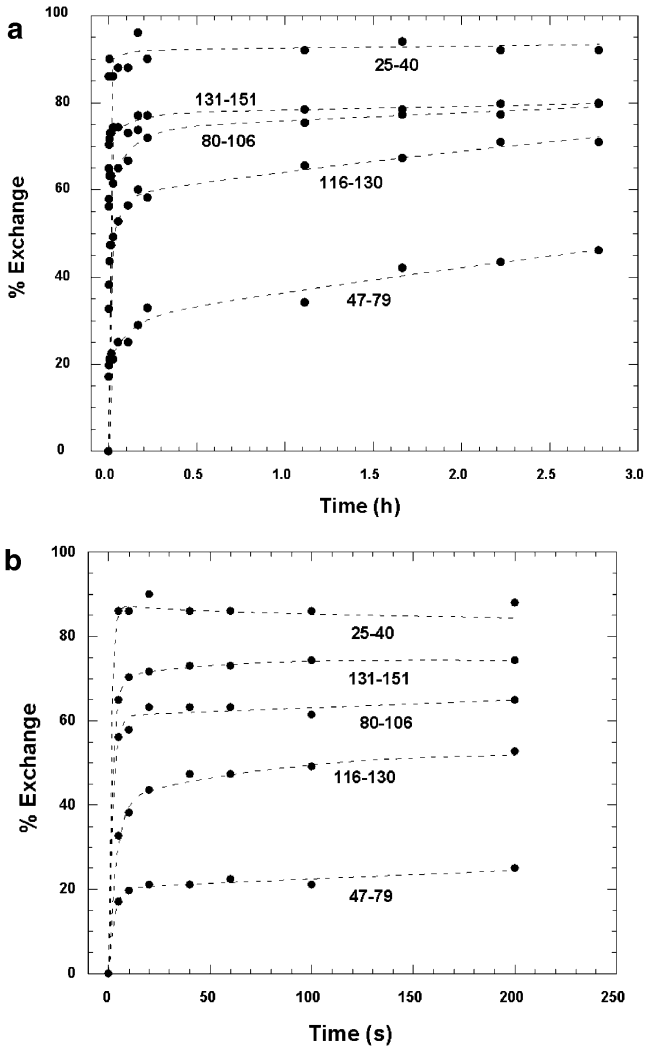

FIGURE 2: (a) Percent H/D exchange *vs* labeling time for representative peptides from HSP16.9 (see Table 1 for other peptides in each rate class). Exchange was carried out at 25 °C and pH 7.0. The lines represent nonlinear least-squares fits to a sum of three exponentials (see the text). (b) Same data as in panel a, shown for the first 200 s only.

Table 1: Number of Fast, Intermediate, and Slow Amide Hydrogens in Peptides Derived from HSP16.9 and Their Associated Rate Constants (*9*)

	fast		intermediate		slow	
peptide	number	k (s^{-1})	number	k (s^{-1})	number	k (s^{-1})
2−16	11	0.49	1	0.004	1	5.0×10^{-5}
17−23	4	0.50	0	−	1	8.6×10^{-5}
24−40	13	0.53	0	−	2	4.7×10^{-5}
25−40	12	>1.00	1	0.002	1	2.3×10^{-5}
41−57	4	>1.00	2	0.003	9	4.8×10^{-5}
47−79	6	0.40	3	0.002	21	2.6×10^{-5}
58−79	4	0.40	4	0.002	12	$<2.0 \times 10^{-5}$
80−106	16	0.50	3	0.002	7	2.2×10^{-5}
97−106	5	0.30	2	0.001	2	$<2.0 \times 10^{-5}$
107−115	4	0.30	1	0.007	3	5.2×10^{-5}
116−130	6	0.30	2	0.005	6	4.0×10^{-5}
131−146	9	0.60	1	0.001	4	2.0×10^{-5}
131−151	13	0.50	1	0.002	4	$<2.0 \times 10^{-5}$

The second fast exchanging region includes residues 131−151. Peptides from this region are ~65% exchanged at 5 s and ~70% exchanged at 10 s. This region includes the C-terminal extension involved in oligomerization. The region

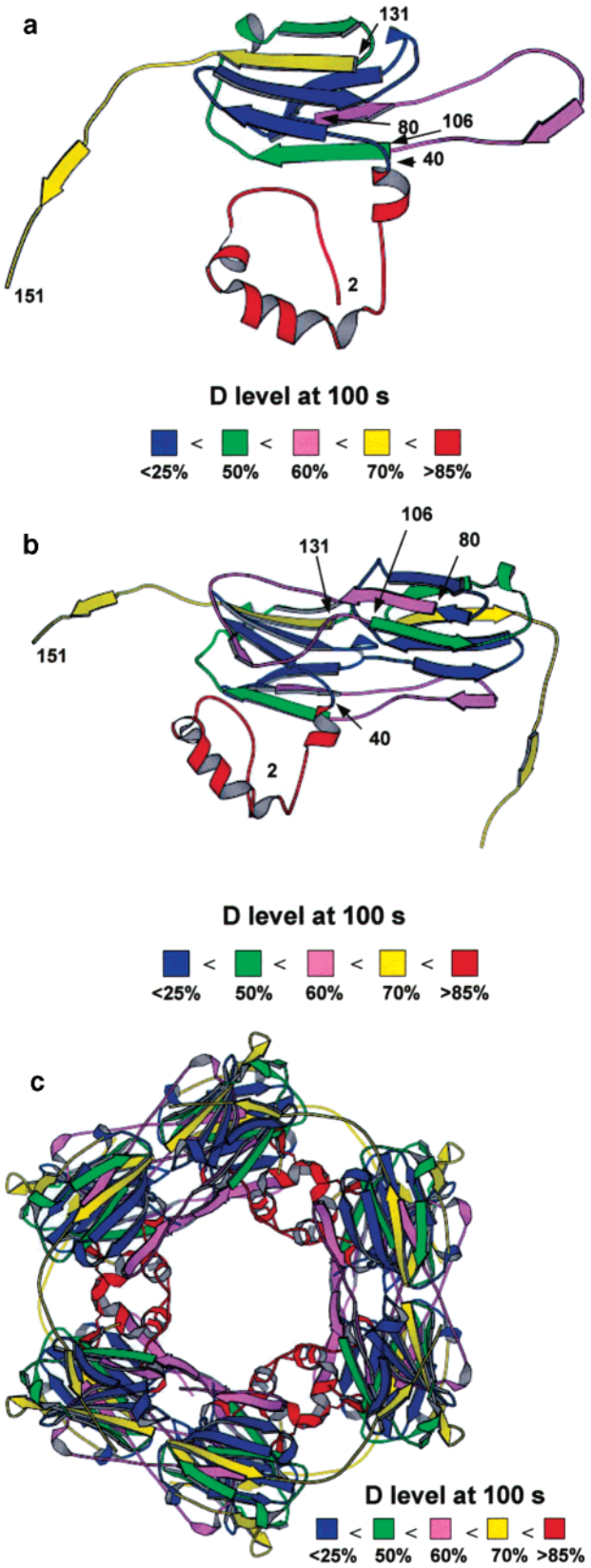

FIGURE 3: (a) Relative exchange behavior (25 °C and pH 7.0) mapped onto the monomer unit of HSP16.9. Note the high solvent accessibility and the lack of structure in the loop formed by residues ~80−106 (magenta). (b) Relative exchange behavior mapped onto the HSP16.9 dimer. Note that the loop of residues 80−106 forms a major portion of the dimer interface. (c) Relative exchange behavior mapped onto the structure of the complete dodecamer.

Table 2: Masses of Peptides Derived from HSP16.9 after Incubation in D_2O for 5 s at 42 °C and for 50 s at 25 °C

peptide	mass at 42 °C	mass at 25 °C	difference
2−16	1744.8	1745.0	−0.2
17−23	854.1	854.0	0.1
24−40	1629.1	1629.7	−0.6
25−40	1481.7	1481.3	0.4
47−79	3738.8	3739.3	−0.5
41−57	2051.4	2051.0	0.4
58−79	2398.0	2398.5	−0.5
80−106	3239.7	3240.6	−0.9
97−106	1206.0	1206.5	−0.5
107−115	1277.6	1277.7	−0.1
116−130	1559.9	1560.3	−0.4
131−146	1730.9	1731.1	−0.2
131−151	2233.8	2233.1	0.7

in which the fewest amide hydrogens undergo exchange, and in which the majority of exchange rates are slow, consists of residues 41−79 and includes the first three β-strands. Peptides from this region are ≤50% exchanged after 2.75 h. Peptides in the region of residues 80−130 exhibit intermediate exchange. Thus, the core, conserved α-crystallin domain shows overall stability compared with the N- and C-terminal regions.

Labeling at 25 and 45 °C. Upon being exposed to temperatures above ~35 °C, HSP16.9 dissociates into assemblies much smaller than the dodecamer (*3*). The structural features of this smaller species, which is believed to be the active, substrate binding form, were determined by comparative labeling of HSP16.9 at 25 and 45 °C. One sample of HSP16.9 was labeled for 50 s at 25 °C. Before the other sample had been labeled at 45 °C, HSP16.9 was incubated in H_2O for 5 min to allow time for conversion of HSP16.9 from the dodecamer to the dissociated species. The dissociated species was then labeled for 5 s in D_2O at 45 °C. The difference in labeling times at the two temperatures compensated for the temperature dependence of the intrinsic rate of H/D exchange (*11*, *12*). The similar deuterium levels of the various peptides after labeling under these conditions (Table 2) demonstrate that exchange patterns at 25 and 45 °C are within experimental error.

Rapid Pulsed Labeling. The 40 N-terminal residues of HSP16.9 show very little protection against H/D exchange after incubation in D_2O for 5 s, even though this region appears to be substantially protected in the crystal structure. A possible explanation is that, in solution, the conformation seen in the crystal structure is in rapid equilibrium with some alternate conformation(s) in which the 40 N-terminal residues are exposed to solvent. To test this hypothesis, HSP16.9 was labeled for 10 ms in an effort to obtain a "snapshot" before major conformational rearrangements were likely to occur.

Although labeling on millisecond time scales is possible using a rapid mixing system, labeling cannot be performed at pH 7.0 because the intrinsic rate of H/D exchange is too slow, and even fully solvent exposed amide hydrogens would remain largely unlabeled after 10 ms (*11*). Effective labeling for very short incubation times requires increasing the intrinsic rate of H/D exchange, which can be accomplished by increasing the pH. The intrinsic rate of H/D exchange is strongly dependent on pH, and this dependence has been quantified in previous NMR studies (*11*). From the data tabulated in Bai and Englander (*11*), it was calculated that

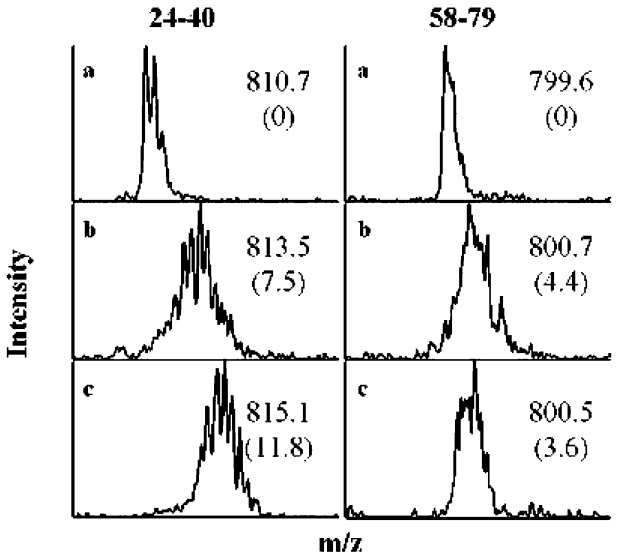

FIGURE 4: Mass spectra for the peptides comprising residues 24−40 and 58−79 after labeling with D_2O at 25 °C for (a) 0 s, (b) 10 ms at pH 9.5, and (c) 5 s at pH 7.0. *m*/*z* values determined from the centroids of the peaks are given. The numbers of deuteriums are indicated in parentheses.

incubation in D_2O for 10 ms at pH 9.5 should result in approximately the same "labeling strength" as incubation for 5 s at pH 7.0, where labeling strength is defined as the labeling time multiplied by the concentration of OH^-. Under both conditions, solvent-exposed amide hydrogens should become almost completely labeled while hydrogen bonded or solvent inaccessible amide hydrogens should remain largely unlabeled. Differences in the deuteration levels that result from labeling under these two conditions should therefore primarily reflect differences in the structure of HSP16.9, and not differences in the labeling conditions.

In the peptides derived from residues 2−40 and 131−151, labeling HSP16.9 at pH 9.5 for 10 ms results in substantially less exchange than labeling for 5 s at pH 7.0. In contrast, peptides from other regions of HSP16.9 exhibit only very small differences in deuteration when labeled under the two conditions. These differences in exchange are evident in Figure 4, which shows data obtained under both labeling conditions for peptide 24−40 from the fast exchanging N-terminus and peptide 58−79 from the slow exchanging core.

Labeling for 10 ms at pH 9.5 and for 5 s at pH 7.0 results in nearly identical mass shifts for peptide 58−79, while peptide 24−40 shows a larger mass shift after 5 s at pH 7.0. Peptides from the region of residues 2−40 exhibit an average level of deuteration of 54% after 10 ms, compared with a level of 85−90% at 5 s, and peptides from the region of residues 131−151 have an average level of deuteration of 45% at 10 ms compared with a level of 65% at 5 s. In terms of the number of deuteriums, peptide 24−40 has gained 7.5 deuteriums after labeling for 10 ms and 11.8 deuteriums after labeling for 5 s. Peptide 58−79 has gained 4.4 deuteriums after 10 ms and 3.6 deuteriums after 5 s. This difference of 0.8 deuterium for peptide 58−79 is slightly greater than the experimental error (repeat measurements on this peptide give a standard deviation of 0.37) and reflects the different labeling conditions that were employed.

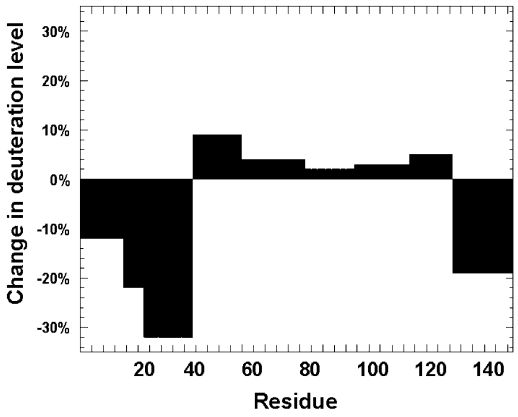

FIGURE 5: Differences in deuterium levels found in peptides derived from HSP16.9 after labeling at 25 °C for 10 ms at pH 9.5 and for 5 s at pH 7.0. Displayed for each peptide is the deuterium level observed at 5 s subtracted from the deuterium level observed at 10 ms.

Differences in deuteration along the HSP16.9 sequence after labeling for 10 ms and 5 s are shown in Figure 5. In contrast to residues 2−40 and 131−151, peptides derived from residues 41−130 exhibit slightly higher levels of deuteration at 10 ms and pH 9.5 than are seen at 5 s and pH 7.0, even though 10 ms at pH 9.5 is a slightly weaker labeling condition than 5 s at pH 7.0. If insufficient labeling strength had resulted in a reduced level of deuterium uptake, we would expect a uniform decrease in the extent of deuteration along the entire sequence of HSP16.9. The fact that a reduced extent of deuteration is seen only in residues 2−40 and 131−151 therefore indicates that it cannot be attributed to insufficient labeling strength and must therefore be attributed to improved protection from exchange as a result of a more structured or solvent-protected environment.

It is a matter of some concern that increasing the pH to 9.5 may induce conformational changes such as partial unfolding. However, high-pH pulsed labeling has been used effectively in a wide range of protein folding studies (*13*−*15*). Furthermore, our results for HSP16.9 show similar deuteration under the two labeling conditions throughout most of the molecule, indicating that major structural features of folded HSP16.9 remain unchanged during the 10 ms exposure to pH 9.5. The significant point of these experiments is that major differences occurred only in those regions involved in maintaining the dodecameric assembly.

DISCUSSION

Gel filtration chromatography and equilibrium analytical ultracentrifugation have shown that, at 25 °C, HSP16.9 exists as a dodecamer in solution (*3*). In the crystal structure of the HSP16.9 dodecameric assembly, residues 1−40 are present as two populations. In half of the monomers, this region exists as three short α-helices which are largely buried and form extensive contacts with monomers from the adjacent ring. In the other half of the monomers, this region does not appear in the electron density, indicating that it is highly dynamic or disordered. The large structural differences of these two populations were expected to lead to bimodal distributions of deuterium that would appear in the mass spectra of peptides from this region as two isotopic envelopes of equal intensity. However, only a single envelope is seen for peptides derived from this region. The deuterium levels of these peptides, ∼85% after 5 s and ∼90% after 10 s, indicate minimal protection. This lack of protection suggests that within 5−10 s the HSP16.9 assembly has undergone conformational changes in which every monomer has exposed its N-terminal region to solvent long enough to become completely exchanged. As judged from the position of these N-terminal regions in the crystal structure, such conformational changes would require substantial disruption of the structure as determined by X-ray crystallography. To expose the amide hydrogens in residues 2−40 for exchange, this region must become fully solvent exposed and the α-helices themselves must unravel to break backbone amide hydrogen bonds. Several scenarios are consistent with the disruption and solvent exposure of the N-terminal region of HSP16.9. It is possible that the N-terminal α-helices break their intersubunit contacts and unravel while remaining largely within the central hole of the dodecamer. This mechanism would require that the remaining intersubunit contacts be sufficient to maintain the structural integrity of the dodecamer. It is also possible that the six structured N-terminal helices trade places with the six unstructured ones on a rapid time scale. Such a rearrangement would involve breaking more intersubunit contacts then simply those formed by the N-terminal residues, and might require the transient formation of additional intersubunit contacts to maintain the dodecameric structure. A third possibility is that exposure of the N-terminal residues for exchange involves partial or complete dissociation of subunits from the dodecamer.

Compared with labeling for 5 s at pH 7.0, labeling for 10 ms at pH 9.5 results in 20−30% less deuterium uptake (i.e., more protection against exchange) in the N-terminal (2−40) and C-terminal (131−151) residues. All other regions of HSP16.9 exhibit slight increases in the level of deuteration for the same labeling conditions. Improved protection on very short time scales is therefore seen only in those regions that form interdimer contacts that are critical for maintaining the structure of the dodecamer. This selective reduction in the rate of deuterium uptake strongly suggests that the N- and C-terminal interactions seen in the crystal structure are maintained on the 10 ms time scale and that, between 10 ms and 5 s, large conformational changes occur that break intersubunit contacts, exposing the N- and C-terminal regions to solvent.

It has been shown that increasing the temperature from 25 to 42 °C causes HSP16.9 to dissociate into subassemblies much smaller than the complete dodecamer. Labeling at 42 °C sheds light on the nature of this suboligomeric form of HSP16.9. Comparing the results of labeling HSP16.9 at 25 and 42 °C shows that the labeling patterns observed at these two temperatures are identical within experimental error. The N- and C-terminal interactions that stabilize the dodecameric structure will presumably be broken when HSP16.9 assumes a suboligomeric form at 42 °C, which is consistent with the lack of protection seen in the N- and C-terminal regions at this temperature. In the structure of the HSP16.9 monomer, the region including residues 80−106 is composed largely of a highly solvent exposed loop (Figure 3a). In the dimer, however, these residues form a major portion of the dimer interface (Figure 3b). If the HSP16.9 subunits seen at high temperatures are free monomers, then amide hydrogens in this region should be almost completely exchanged within the first few seconds of incubation in D_2O. The fact that

peptides from this region exhibit substantial protection at both 25 and 42 °C strongly suggests that the dimer interface is preserved when the dodecamer dissociates into subunits, and that these subunits are in fact free dimers.

It is useful to consider the results of the present H/D exchange study in the context of previous work on subunit exchange between HSP16.9 and HSP18.1, particularly the recent results of Sobott *et al*. (*6*). They found that hybrid assemblies appear within ~1 min of initiation of incubation of the two HSPs together. In discussing the crystal structure of HSP16.9, van Monfort *et al*. (*3*) noted that this rapid subunit exchange is in striking contrast to the extensive interactions that maintain the dodecameric structure (*3*). H/D exchange reveals that these extensive interactions are not stable in solution but are broken on a rapid (subsecond) time scale, and that protein regions participating in these interactions spend a significant fraction of time in an unstructured state. The unexpectedly labile nature of the intersubunit interactions should facilitate the exit of subunits from the dodecamer. Thus, the H/D exchange results rationalize the apparent discrepancy between the extensive intersubunit interactions seen in the crystal structure of HSP16.9 and the rapid subunit exchange that is seen in solution. Sobott *et al*. (*6*) also found that, during the first few minutes of subunit exchange, the major species in solution are assemblies that have swapped two monomers, suggesting that dimers remain intact during the initial subunit exchange process. This is consistent with our observation that the dimer interface of HSP16.9 exhibits substantial protection, even at 42 °C when the protein exists in a subdodecameric form. Both the results of Sobott *et al*. and the results from H/D exchange indicate that the HSP16.9 dimer remains stable upon removal from the dodecamer.

For several sHSPs, studies have shown that temperature activation results in the exposure of hydrophobic surface area (*4*, *5*, *16*), and it is thought that this newly exposed surface area is involved in substrate binding. From our H/D exchange results, it appears that the exposure of this surface area occurs when a subunit is released from the assembly. The newly exposed hydrophobic surface area might result from the unwinding of the N-terminal helices, or it might result from the exposure of other parts of the dimer surface that are not solvent accessible in the dodecamer. Importantly, our data show that increased temperatures and the consequent release of free dimers do not appear to induce any additional structural changes beyond those that result from the dissociation of the dodecamer; the core α-crystallin domain remains structurally intact. Thus, our results suggest that heat activation of HSP16.9 is accomplished primarily by shifting the equilibrium from favoring the dodecamer to favoring free subunits.

Although free subunits will predominate only at elevated temperatures, rapid subunit exchange occurs at room temperature (*6*). It is interesting to speculate about possible functional roles for the rapid subunit dynamics observed at room temperature. Several other small heat shock proteins, including α-crystallin, undergo subunit exchange (*17*, *18*). While a number of studies have documented the fact that high temperatures cause structural changes in α-crystallin that are correlated with enhanced chaperone-like activity (*4*, *19*, *20*), other studies indicate that α-crystallin chaperone-like activity is not strictly dependent on increased temperature (*21*, *22*). A reduced level of subunit exchange in α-crystallin also appears to reduce chaperone-like activity (*23*). These results suggest that rapid quaternary structure dynamics may be important for the functioning of sHSPs at room temperature. sHSPs are known to have physiological roles in addition to offering protection from heat stress. sHSPs have been shown to associate with the cytoskeleton during cell morphogenesis, and are thought to play a role in stabilizing actin filaments (*24*, *25*). Additionally, sHSPs have recently been implicated in the regulation of apoptosis (*26*). Maintaining a fast dynamic equilibrium between the dodecameric assembly and free dimers may allow sHSPs to respond rapidly to changing cellular conditions.

REFERENCES

1. Van Monfort, R., Slingsby, C., and Vierling, E. (2002) *Adv. Protein Chem. 59*, 105−156.
2. Torok, Z., Goloubinoff, P., Tsvetkova, N., Glatz, A., Balogh, G., Varvasovszki, V., Los, D., Vierling, E., Crowe, J., and Vigh, L. (2001) *Proc. Natl. Acad. Sci. U.S.A. 98*, 3098−3103.
3. Van Monfort, R., Basha, E., Friedrich, K., Slingsby, C., and Vierling, E. (2001) *Nat. Struct. Biol. 8*, 1025−1030.
4. Rao, C. M., Raman, B., Ramakrishna, T., Rajaraman, K., Ghosh, D., Datta, S., Trivedi, V. D., and Sukhaswami, M. B. (1998) *Int. J. Biol. Macromol. 22*, 271−281.
5. Lee, G. J., Roseman, A. M., Saibil, H. R., and Vierling, E. (1997) *EMBO J. 16*, 659−671.
6. Sobott, F., Benesch, J., Vierling, E., and Robinson, C. V. (2002) *J. Biol. Chem. 277*, 38921−38929.
7. Englander, S. W., Mayne, L., Bai, Y., and Sosnick, T. R. (1997) *Protein Sci. 6*, 1101−1109.
8. Bai, Y., and Englander, S. W. (1996) *Proteins: Struct., Funct., Genet. 24*, 145−151.
9. Zhang, Z., and Smith, D. L. (1993) *Protein Sci. 2*, 522−531.
10. Lee, G. J., Pokala, N., and Vierling, E. (1995) *J. Biol. Chem. 270*, 10423−10438.
11. Bai, Y., Milne, J. S., Mayne, L., and Englander, S. W. (1993) *Proteins: Struct., Funct., Genet. 17*, 75−86.
12. Liu, Y., and Smith, D. L. (1994) *J. Am. Soc. Mass Spectrom. 5*, 19−28.
13. Udgaonkar, J. B., and Baldwin, R. L. (1988) *Nature 335*, 694−699.
14. Englander, S. W., and Mayne, L. (1992) *Annu. Rev. Biophys. Biomol. Struct. 21*, 243−265.
15. Yang, H., and Smith, D. L. (1997) *Biochemistry 36*, 14992−14999.
16. Haslbeck, M., Stromer, W. S., Ehrnsperger, M., White, H. E., Chen, S. X., and Bucher, J. (1999) *EMBO J. 18*, 6744−6751.
17. Bova, M., Ding, L., Horwitz, J., and Fung, B. (1997) *J. Biol. Chem. 272*, 29511−29517.
18. Bova, M., Huang, Q., Ding, L., and Horwitz, J. (2002) *J. Biol. Chem. 277*, 38468−38475.
19. Datta, S. A., and Rao, C. M. (1999) *J. Biol. Chem. 274*, 34773−34778.
20. van Boekel, M. A. M., deLange, F., de Grip, W. J., and de Jong, W. W. (1999) *Biochim. Biophys. Acta 1434*, 114−123.
21. Bhattacharyya, J., and Das, K. (1998) *Biochem. Mol. Biol. Int. 46*, 249−258.
22. Lindner, R. A., Kapur, A., Mariani, M., Titmuss, S. J., and Carver, J. A. (1998) *Eur. J. Biochem. 258*, 170−183.
23. Liang, J., and Fu, L. (2002) *Biochem. Biophys. Res. Commun. 293*, 7−12.
24. Piotrowicz, R., and Levin, E. (1997) *J. Biol. Chem. 272*, 25920−25927.
25. Minowada, G., and Welch, W. (1995) *J. Biol. Chem. 270*, 7047−7054.
26. Xanthoudakis, S., and Nicholson, D. W. (2000) *Nat. Cell Biol. 2*, E164−E165.

BI034117M